



Compact binary merger and kilonova: outflows from remnant disc

Tuan Yi,¹ Wei-Min Gu,^{1,2★} Tong Liu,¹ Rajiv Kumar,¹ Hui-Jun Mu¹
and Cui-Ying Song¹

¹Department of Astronomy, Xiamen University, Xiamen, Fujian 361005, China

²Jiujiang Research Institute of Xiamen University, Jiujiang 332000, China

Accepted 2018 January 26. Received 2018 January 26; in original form 2017 October 24

ABSTRACT

Outflows launched from a remnant disc of compact binary merger may have essential contribution to the kilonova emission. Numerical calculations are conducted in this work to study the structure of accretion flows and outflows. By the incorporation of limited-energy advection in the hyper-accretion discs, outflows occur naturally from accretion flows due to imbalance between the viscous heating and the sum of the advective and radiative cooling. Following this spirit, we revisit the properties of the merger outflow ejecta. Our results show that around $10^{-3} \sim 10^{-1} M_{\odot}$ of the disc mass can be launched as powerful outflows. The amount of unbound mass varies with the disc mass and the viscosity. The outflow-contributed peak luminosity is around $10^{40} \sim 10^{41} \text{ erg s}^{-1}$. Such a scenario can account for the observed kilonovae associated with short gamma-ray bursts, including the recent event AT2017gfo (GW170817).

Key words: accretion, accretion discs – black hole physics – binaries: close – gamma-ray burst: general – stars: winds, outflows.

1 INTRODUCTION

The study of the origin of short-duration gamma-ray bursts (SGRBs) is of great importance in astrophysics. This high energy astrophysical phenomenon, as a subclass of gamma-ray bursts (GRBs), is characterized by their intense flux of gamma-ray photons in only up to a few seconds (typically less than two seconds). Therefore, it must conceal the most violent activities at its very centre. It is commonly believed that SGRBs could be powered by the accretion of the remnant disc after the coalescence of compact binaries (e.g. Narayan, Paczynski & Piran 1992; Nakar 2007; Berger 2014), either double neutron star (NS–NS) binaries or black hole–neutron star (BH–NS) binaries. A recent inspiring progress is the detection of the gravitational wave (GW) event GW170817 from binary NS merger (Abbott et al. 2017a) and a coincident short-GRB 170817A (Abbott et al. 2017b; LIGO Scientific Collaboration et al. 2017a, also observed from the all bands of the electromagnetic radiation).

The merger of compact binaries with at least one NS may be accompanied with radioactive decay of r-process elements (rapid neutron capture nucleosynthesis), which is known as kilonova/macronova. (e.g. Li & Paczyński 1998; Metzger et al. 2010; Metzger & Berger 2012; Jin et al. 2013; Kasen, Badnell & Barnes 2013; Tanaka & Hotokezaka 2013; Yu, Zhang & Gao 2013; Gao et al. 2015; Kasen, Fernández & Metzger 2015; Rosswog 2015; Kawaguchi et al. 2016; Tanaka 2016; Chornock et al. 2017; Drout et al. 2017; Evans et al. 2017; Fernández et al. 2017; Li et al.

2017; The LIGO Scientific Collaboration et al. 2017b; Metzger 2017; Murguía-Berthier et al. 2017b; Tanaka et al. 2017). The first confirmed kilonova is associated with GRB 130603B (Tanvir et al. 2013; Berger, Fong & Chornock 2013; Fan et al. 2013), which is about 1000 times brighter than the nova (hence named ‘kilonova’ by Metzger et al. 2010), 10 to 100 times fainter than the supernova. These events have long afterglow in optical band for several hours to days (up to a week). For example, the optical transient coincident with GW170817 was found by the Swope Telescope (SSS17a Coulter et al. 2017), with a total radiated energy of $1.7 \times 10^{47} \text{ erg}$ over 18 d (Drout et al. 2017).

The basic ingredients that power the kilonova are the central compact object and the ejected materials (ejecta). The merger can result in a stellar-mass BH surrounded by a remnant disc (torus) or a magnetar (e.g. Duncan & Thompson 1992; Usov 1992; Dai & Lu 1998; Dai et al. 2006; Metzger et al. 2011; Lü et al. 2015), both of which can eject neutron rich materials. For instance, the kilonova produced by GW170817 has ejected $\gtrsim 10$ per cent ($10^{-3} \sim 10^{-2} M_{\odot}$) of the matter from the merger (The LIGO Scientific Collaboration et al. 2017b). The ejecta can generally be classified into two types (Fernández & Metzger 2016): (i) dynamical ejecta originates from the tidal tail of the BH–NS merger or the heating by shock interface of the NS–NS merger; (ii) outflows/wind that arises from the remnant disc. As pointed by Metzger (2017), ejecta from outflows can rival or even dominate over the dynamical ejecta.

The remnant disc launching such outflows/wind has the following properties: (i) extremely high accretion rates ($10^{-3} M_{\odot} \text{ s}^{-1} \lesssim \dot{M} \lesssim 10 M_{\odot} \text{ s}^{-1}$); (ii) extremely high density ($\rho \sim 10^8 \sim 10^{12} \text{ g cm}^{-3}$) and high temperature ($T \sim 10^{10} \sim 10^{11} \text{ K}$). Popham, Woosley &

* E-mail: guwm@xmu.edu.cn

Fryer (1999) studied this kind of accretion flows and found that the neutrino emission dominates the cooling of the flow due to the annihilation of neutrino and antineutrino pairs. The annihilation could give rise to an energy output up to 10^{52} erg s $^{-1}$, which is enough to power the observed SGRBs. They named such flows as neutrino-dominated accretion flows (NDAFs; also known as the neutrino-cooled discs). For more details on structure and properties of the NDAFs, one can refer to the works: Popham et al. (1999), Narayan, Piran & Kumar (2001), Di Matteo, Perna & Narayan (2002), Kohri & Mineshige (2002), Kohri, Narayan & Piran (2005), Gu, Liu & Lu (2006), Liu et al. (2007), Chen & Beloborodov (2007), Kawanaka & Kohri (2012), Kawanaka, Piran & Krolik (2013), Zalamea & Beloborodov (2011), Xue et al. (2013), Cao, Liang & Yuan (2014), Xie, Lei & Wang (2016), or a recent review Liu, Gu & Zhang (2017).

Outflows exist in many accretion systems such as low-mass X-ray binaries (Fender et al. 2004) and active galactic nuclei (Terashima & Wilson 2001; Ganguly & Brotherton 2008; Pounds & Reeves 2009). For example, our Galactic Centre Sgr A* harbors a supermassive BH (SMBH) of 3.6 million solar masses, and more than 99 per cent of the accreted mass escape from the surrounding disc according to observations (Wang et al. 2013). Magneto-hydrodynamical (MHD) simulations have found that outflows exist in both optically thin flows (Yuan, Wu & Bu 2012a; Yuan, Bu & Wu 2012b) and optically thick flows (Jiang, Stone & Davis 2014; Sądowski & Narayan 2015, 2016). Recent simulations by Jiang, Stone & Davis (2017) have found that outflows are formed with speed $v_{\text{out}} \sim 0.1\text{--}0.4c$ for super-Eddington accretion discs around SMBHs. For the hyper-accretion disc, recent three-dimensional general-relativistic MHD (GRMHD) simulations by Siegel & Metzger (2017) have shown that about 20 per cent of the initial torus mass is unbound and form powerful outflows with speed $v_{\text{out}} \sim 0.03\text{--}0.1c$. The outflows can be driven by the gradient of the gas pressure, the radiation pressure (Proga 2003; Ohsuga 2007), or the magnetic pressure (Samadi & Abbassi 2016). In addition, outflows may be driven by neutrino pressure (Perego et al. 2014; Murguía-Berthier et al. 2017a) at extremely high accretion rates ($\dot{M} \gtrsim 1 M_{\odot} \text{ s}^{-1}$). On the other hand, Gu (2015) proposed that for the case of low radiative cooling efficiency, outflows should occur inevitably owing to the limited-energy advection, no matter the flow is optically thin or thick. A similar issue on the outflows of radiation-pressure supported accretion disc was investigated by Gu (2012).

In this work, the central engine powering the kilonova associated with SGRBs is revisited. For the first time, we incorporate the limited-energy advection within NDAFs. Consequently, the outflows can be naturally launched from the hyperaccretion disc. In Section 2, our model is presented to describe the central engine of kilonova. Numerical results and analyses are presented in Section 3. Discussion of implications and applications of our model are made in Section 4.

2 THEORETICAL MODEL

Fig. 1 is an illustration of the NS–NS/BH–NS merger and the remnant disc formed after the binary merger. Bipolar jet is launched by the Blandford–Znajek (BZ) process (Blandford & Znajek 1977). In the inner part of the accretion disc, the neutrino–antineutrino annihilation leads to a large amount of neutrino radiation. These two mechanisms are believed to be the possible energy source of the GRBs (e.g. Liu et al. 2015; Song et al. 2015, 2016). Outflows from the disc can supply the neutron rich materials for the generation of kilonova.

In the present work, the accretion disc is assumed to be steady and axisymmetric, surrounding the merged BH. The pseudo-Newtonian potential is adopted to describe the spacetime around the BH, $\Psi = -GM_{\text{BH}}/(R - R_g)$ (Paczynsky & Wiita 1980), where M_{BH} is the BH mass, and $R_g = 2GM_{\text{BH}}/c^2$ is the Schwarzschild radius.

In order to examine the outflows from the disc, the equations of continuity, motion, energy, and the equation of state are assembled to describe the accretion flows. The continuity equation is

$$\dot{M} = -4\pi\rho H R v_R, \quad (1)$$

where \dot{M} is the accretion rate, ρ the density, H the half thickness of the disc, and v_R the radial velocity. The equation of motion has three components. For the radial momentum equation we assume

$$\Omega = \Omega_K = \frac{1}{R - R_g} \sqrt{\frac{GM_{\text{BH}}}{R}}, \quad (2)$$

with Ω_K being the Keplerian angular velocity. The hydrostatic balance in the vertical direction takes as the usual simplified form:

$$H = \frac{c_s}{\Omega_K}, \quad (3)$$

where $c_s = \sqrt{P/\rho}$ is the isothermal sound speed, with P being the total pressure. The azimuthal momentum can be simplified as (Gu et al. 2006)

$$v_R = -\alpha c_s \frac{H}{R} f^{-1} g, \quad (4)$$

where $g = -d \ln \Omega_K / d \ln R$ and $f = 1 - j/\Omega_K R^2$, with j being the specific angular momentum per unit mass accreted by the BH. α is the viscous parameter.

The equation of state is (e.g. Di Matteo et al. 2002)

$$P = P_{\text{gas}} + P_{\text{rad}} + P_{\text{deg}} + P_{\nu}, \quad (5)$$

where the total pressure P is composed of the gas pressure P_{gas} , radiation pressure of photons P_{rad} , degenerate pressure of electrons P_{deg} , and the radiation pressure of neutrinos P_{ν} . The equation of energy is expressed as

$$Q_{\text{vis}} = Q_{\text{adv}} + Q_{\nu} + Q_{\text{out}}. \quad (6)$$

This equation shows the balance between the viscous heating Q_{vis} and the sum of advective cooling Q_{adv} , neutrino cooling Q_{ν} , and the cooling due to outflows Q_{out} . The expressions of P_{gas} , P_{rad} , P_{deg} , P_{ν} , Q_{vis} , Q_{adv} , and Q_{ν} can be found in the previous paper Yi et al. (2017). One can refer to Popham & Narayan (1995); Di Matteo et al. (2002); Kohri et al. (2005), for more physics of the neutrino-cooled disc described by the equations.

As mentioned in Section 1, Gu (2015) studied the accretion flows by comparing the vertically integrated advection cooling rate with the viscous heating rate, the former is found to be generally less than 30 per cent of the latter. This hints that the outflows should rise up naturally to balance the heating owing to the limited-energy advection and radiation. This constraint is adopted in our analyses and calculations. We define $f_{\text{adv}} = Q_{\text{adv}}/Q_{\text{vis}}$ as the advection factor, $f_{\nu} = Q_{\nu}/Q_{\text{vis}}$ the neutrino cooling factor, and $f_{\text{out}} = Q_{\text{out}}/Q_{\text{vis}}$ the outflows factor. These factors compete each other to gain the balance in the accretion flows. The maximum value of f_{adv} is set to be 0.2, which restricts the advection portion, and therefore the excess viscous heating energy will be dispensed to the outflows.

The standard α -disc prescription (Shakura & Sunyaev 1973) is adopted in this work, namely the kinematic viscosity coefficient $\nu = \alpha c_s H$. The viscous parameter α is subject to uncertainty (Potter & Balbus 2014), so the dependence of the results to α is

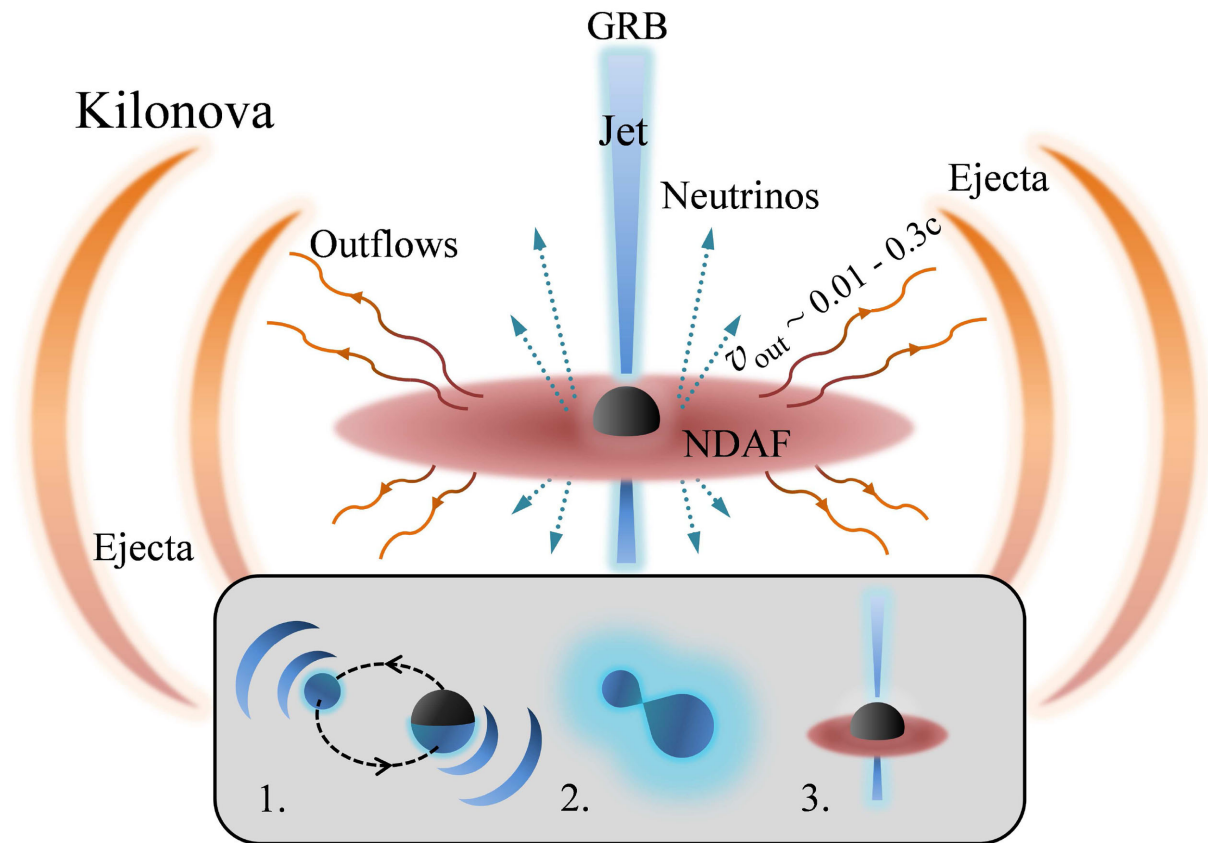


Figure 1. Illustration of a compact binary merger (NS–NS/BH–NS binary) with strong outflows that powers a kilonova. 1. Pre-merger stage, the binary with GW emission. 2. The coalescence of the binary. 3. The formation of a hyperaccretion disc around the BH after the merger.

studied in this work. Since the quantities in equations (1)–(6) are functions of temperature T and density ρ , with the given parameters M_{BH} , j , \dot{M} , and α , the profiles of T and ρ can be evaluated at each point along the radius. The mass of central BH is taken to be $M_{\text{BH}} = 3 M_{\odot}$, the specific angular momentum $j = 1.83 c R_g$ (close to the Keplerian angular momentum at the marginally stable orbit $l_{\text{K}|3R_g} = 1.837 c R_g$), and the accretion rate is set in the range $10^{-2} M_{\odot} \text{ s}^{-1} \lesssim \dot{M} \lesssim 10 M_{\odot} \text{ s}^{-1}$. Four different values of viscous parameter are examined, i.e. $\alpha = 0.01, 0.02, 0.05$, and 0.1 .

3 NUMERICAL RESULTS

3.1 Outflow regions and strength

In this section, we present numerical results of the accretion flows with outflows. Outflows were ignored in most previous works on NDAFs (e.g. Popham et al. 1999; Narayan et al. 2001; Di Matteo et al. 2002; Kohri & Mineshige 2002; Gu et al. 2006). When the energy equilibrium is re-examined with limited-energy advection, i.e. the balance of equation (6), we can find the regions where outflows ought to occur. As shown in Fig. 2 where $\alpha = 0.02$ is adopted (Hirose, Blaes & Krolik 2009), for a given mass accretion rate \dot{M} , the flow can be divided into three regions by two critical radii R_{c1} and R_{c2} . The inner and outer regions (grey) correspond to the cases that outflows ought to occur, whereas the middle region (sky blue) corresponds to the cases that the sum of neutrino cooling and advective cooling can balance the viscous heating, therefore

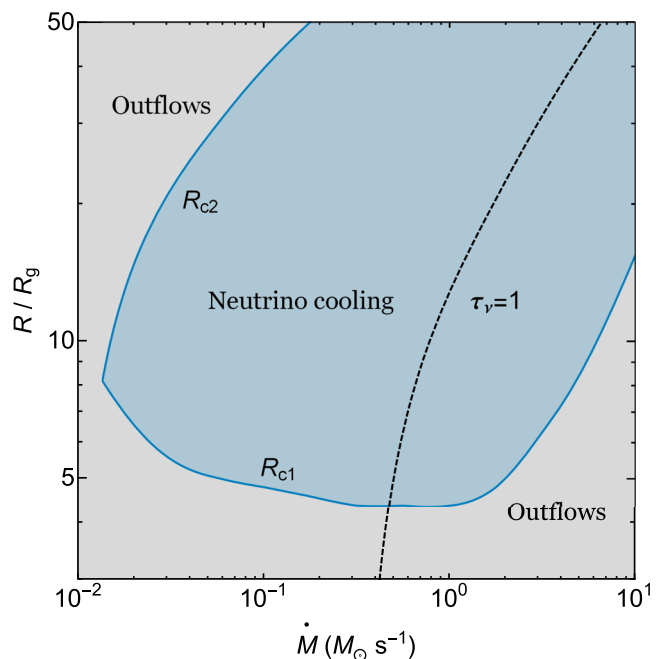


Figure 2. The neutrino cooling region (sky blue) and the outflows region (grey) for different accretion rates, where $\alpha = 0.02$ is adopted. The black dashed line represents the photosphere for the neutrinos.

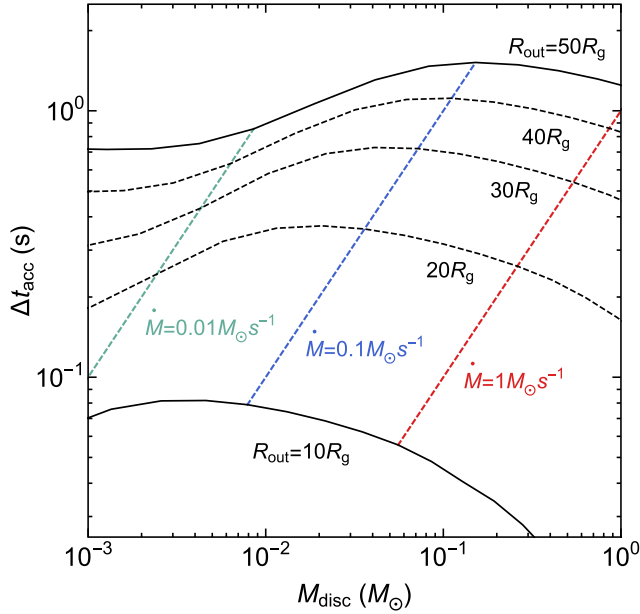


Figure 3. The estimated accretion time-scales for discs with different masses, sizes, and accretion rates, where $\alpha = 0.02$.

outflows are not necessary. The black dashed line represents the photosphere where the optical depth for the neutrinos equals unity. The physics behind the figure is that, for low accretion rates the outer part of the disc has relatively low density and temperature. In such case, the neutrino cooling is quite inefficient. In addition, as mentioned in Section 1, the energy advection is also limited. Thus, the sum of the neutrino cooling and the advective cooling cannot balance the viscous heating, and therefore outflows will be launched and take away part of the viscous heating. On the other hand, for high accretion rates ($\dot{M} \gtrsim 1 M_\odot \text{ s}^{-1}$), neutrino emission becomes much stronger, but the inner part of the disc becomes optically thick to neutrinos, so a considerable amount of neutrinos will be trapped. Thus, the efficiency of neutrino cooling is low compared to the large viscous heating. As a consequence, the outflows at the inner part of the disc will be enhanced.

In order to calculate the energy carried along the outflows, the accretion discs for different masses and sizes are considered to estimate the accretion time-scales. The mass of the disc M_{disc} is related to the total mass and the mass ratio of the binary, it can also be altered by the dynamical process of the merger. Shen et al. (2017) discussed the possible value of M_{disc} and suggested an upper limit of $M_{\text{disc}} \lesssim 0.3 M_\odot$. Numerical simulations by Just et al. (2015b) found a similar range of 0.03–0.3 M_\odot . Typically the disc will extend itself up to a few hundred kilometres from the centre (Siegel & Metzger 2017).

The outer boundary of the disc radius is set in the range of $10 R_g \leq R_{\text{out}} \leq 50 R_g$, while the accretion rate \dot{M} is taken from 10^{-3} – $10 M_\odot \text{ s}^{-1}$. Thus the masses of the disc can be calculated by the radial integration of the density. The time-scale of the accretion can then be estimated by

$$\Delta t_{\text{acc}} \approx \int_{R_{\text{in}}}^{R_{\text{out}}} -\frac{1}{v_R} dR = \frac{M_{\text{disc}}}{\dot{M}}. \quad (7)$$

The outflows will take launch within Δt_{acc} , before the remnant disc is exhausted. Fig. 3 shows the variation of Δt_{acc} with respect to M_{disc} . Two black solid lines mark the range of the disc radius ($10 R_g$ and $50 R_g$), and black dashed lines mark three typical radii in

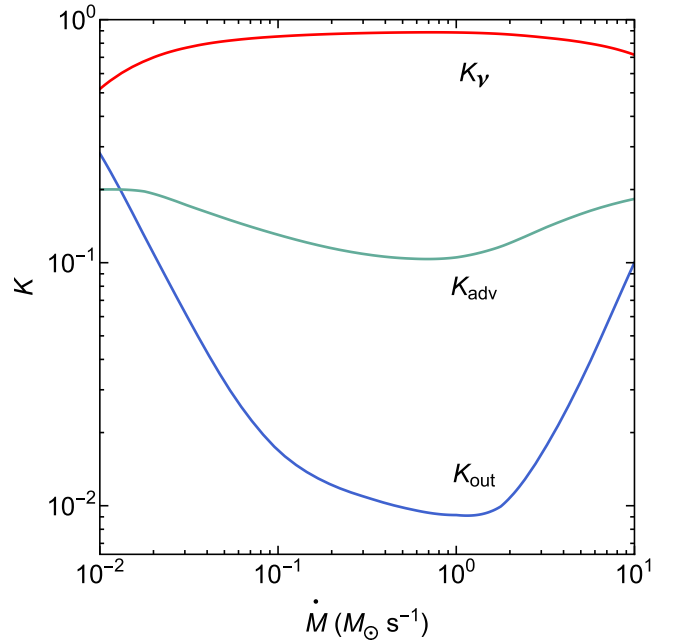


Figure 4. Variations of the total outflow, advection, and neutrino cooling factors with respect to \dot{M} , where $R_{\text{out}} = 50 R_g$ and $\alpha = 0.02$.

between. Three dashed colour lines represent the results for $\dot{M} = 0.01$ (green), $\dot{M} = 0.1$ (blue), and $1 M_\odot \text{ s}^{-1}$ (red). The results show that the accretion time-scales vary from a few tens of milliseconds up to around two seconds, which are consistent with the durations of typical SGRBs ($\lesssim 2 \text{ s}$).

With known masses, sizes, accretion durations, and outflows regions of the discs, the energy carried away by the outflows can be investigated in the first place. The total viscous heating can be evaluated by the radial integration of the viscous heating:

$$A_{\text{vis}} = \int_{R_{\text{in}}}^{R_{\text{out}}} 4\pi R \cdot Q_{\text{vis}} dR \approx \frac{1}{16} \dot{M} c^2. \quad (8)$$

The dimensionless total cooling rate factors are defined as: $K_v = \int_{R_{\text{in}}}^{R_{\text{out}}} 4\pi R \cdot Q_v dR / A_{\text{vis}}$, $K_{\text{adv}} = \int_{R_{\text{in}}}^{R_{\text{out}}} 4\pi R \cdot Q_{\text{adv}} dR / A_{\text{vis}}$, and $K_{\text{out}} = \int_{R_{\text{in}}}^{R_{\text{out}}} 4\pi R \cdot Q_{\text{out}} dR / A_{\text{vis}}$, for neutrinos, advection, and outflows, respectively.

Fig. 4 shows the variation of K_v (red line), K_{adv} (green line), and K_{out} (blue line) with respect to \dot{M} . The size of the disc is taken to be $50 R_g$. As shown in the figure, the neutrino cooling is the highest for all given accretion rates, the advective cooling is in between, and the outflows is the lowest. The outflows possess a relatively large fraction (~ 10 per cent) at low and high ends of the accretion rate. The overall outflows factor is around $10^{-2} \sim 10^{-1}$. Even at its minimum, about 1 per cent of the viscous heating is taken by the outflows. It is a significant amount of energy as you will see in the following analyses.

3.2 Outflow-contributed materials and energy

In this section, we revisit the properties of the outflow component of the kilonova. The goal is to estimate the mass of outflows ejecta and its contribution to the luminosity. The calculations are organized as follows. Step (1): The disc outflow masses M_{out} are calculated. It is derived by the kinetic energy ($E_{\text{out}} = \frac{1}{2} M_{\text{out}} v_{\text{out}}^2$) and assumed velocities (v_{out}) of the outflows. The dependence of the outflow mass to different disc mass M_{disc} and viscous parameter α is investigated.

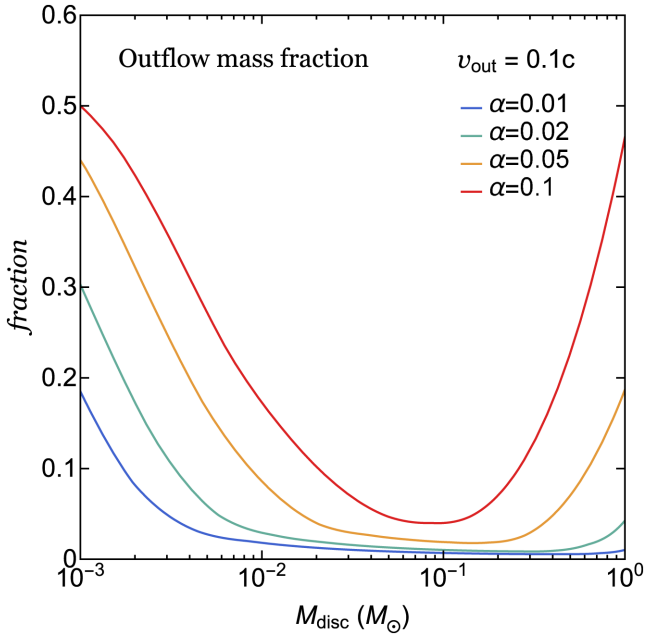


Figure 5. Variations of the outflow mass fraction with the disc mass. Colour lines represent results for $\alpha = 0.01$ (blue), 0.02 (green), 0.05 (orange), and 0.1 (red).

Step (2): The peak luminosity L_{peak} of the kilonova emission is calculated by adopting the one-zone expanding envelope model (Li & Paczyński 1998). The impacts of M_{out} , v_{out} , and α to L_{peak} are studied. In addition, the influence of the opacity κ is briefly discussed.

The kinetic energy E_{out} is different from the total outflows energy. A part of the latter is required to free materials from central potential well. Hence E_{out} equals the total outflows energy minus the binding energy of the flow. Thus, the following equation holds:

$$\frac{1}{2} M_{\text{out}} v_{\text{out}}^2 = \int_{R_{\text{in}}}^{R_{\text{out}}} 4\pi R \cdot Q_{\text{out}} dR \times \Delta t_{\text{acc}} - \eta M_{\text{out}} c^2, \quad (9)$$

where Q_{out} is computed by equation (6). The dimensionless factor η denotes the fraction of the rest mass energy that is stored as the binding energy of the flow. Equation (9) can be easily solved for different outflows velocities v_{out} . The domain $0.01 \sim 0.3c$ for v_{out} is investigated. (Drout et al. 2017; Fujibayashi et al. 2017; Siegel & Metzger 2017).

The total outflows energy is obtained by integrating the Q_{out} from the marginally stable orbit $3R_g$ to the outer boundary R_{out} . We choose $\eta \approx 1/16$ due to the Paczyński–Wiita potential. The unbound mass is found in the range $10^{-3} \sim 10^{-1} M_{\odot}$. The outflow mass fraction ($M_{\text{out}}/M_{\text{disc}}$) relies on M_{disc} and α . The results are shown in Fig. 5, with a typical outflow velocity $v_{\text{out}} = 0.1c$ and a typical outer boundary $R_{\text{out}} = 20R_g$. For low-mass remnant disc with $M_{\text{disc}} \lesssim 0.1 M_{\odot}$, the fraction increases with decreasing M_{disc} . If M_{disc} goes down to $\sim 10^{-3} M_{\odot}$, more than 30 per cent of the disc materials can be launched as the form of outflows. But the fraction heavily depends on the viscosity α . The influence of α is indicated by the colour lines. If α is larger, more materials tend to be pushed away. For larger remnant discs with $M_{\text{disc}} \gtrsim 0.1 M_{\odot}$, the outflows possess a relatively small mass fraction $\lesssim 10$ per cent. The viscosity has relatively mild effects on the flow. The dependence of the results to α can be understood in the following way. According to equation (4), large α means large radial velocity. As a consequence, the ratio of the advective cooling to the neutrino cooling becomes

large. However, due to the limited-energy advection, a large amount of energy stored in the accretion flow ought to be released through outflows. Thus, for larger viscous parameter, the fraction of energy owing to outflows is also larger, and therefore the outflow mass fraction becomes larger.

The amount of merger outflows has been investigated by many simulations (e.g. Fernández & Metzger 2013; Just et al. 2015a; Fujibayashi et al. 2017; Shibata et al. 2017; Siegel & Metzger 2017). Despite of different parameters were assumed among those simulations, the outflow mass fraction was found in the range 5 per cent \sim 30 per cent. As shown in Fig. 5, our results are roughly in agreement with the simulation results. For instance, in the GRMHD simulations of Siegel & Metzger (2017), a torus of $0.02 M_{\odot}$ will lose 16 per cent of the materials through outflows, and our calculations found that the value is ~ 10 per cent in the similar circumstances. The quantitative difference between our results and the simulations may be related to the different outer boundaries and outflow velocities. Moreover, our results are based on a fixed upper limit of energy advection $f_{\text{adv}}^{\text{max}} = 0.2$. However, the previous analyses (Gu 2015) indicate a flexible upper limit, i.e. $f_{\text{adv}}^{\text{max}} \lesssim 0.3$, which can have quantitative influence on the results. In addition, the magnetic fields are not taken into consideration in this work, which may also have effects on our results.

The kilonova ejecta can be simplified as spherically, uniformly expanding layers of neutron rich materials. (Li & Paczyński 1998; Metzger et al. 2010; Kasen et al. 2013; Tanaka & Hotokezaka 2013; Rosswog 2015; Fernández & Metzger 2016; Tanaka 2016; Metzger 2017). The peak luminosity of the radioactive decay is given by (Tanaka 2016)

$$L_{\text{peak}} = 1.3 \times 10^{40} \text{ erg s}^{-1} \times \left(\frac{\epsilon_{\text{dep}}}{0.5} \right)^{1/2} \left(\frac{M_{\text{ejec}}}{0.01 M_{\odot}} \right)^{0.35} \times \left(\frac{v}{0.1c} \right)^{0.65} \left(\frac{\kappa}{10 \text{ cm}^2 \text{ g}^{-1}} \right)^{-0.65}, \quad (10)$$

where $\epsilon_{\text{dep}} < 1$ is the fraction of energy deposition. A typical value 0.5 for ϵ_{dep} is taken. M_{ejec} is specified as the outflows ejecta mass M_{out} in the calculation. κ is the opacity of the outflows. The value of κ is uncertain due to the complexity of the outflow composition (Barnes & Kasen 2013).

Fig. 6 shows the variations of L_{peak} with respect to v_{out} . Three typical disc masses are examined, i.e. $M_{\text{disc}} = 0.03 M_{\odot}$ (green), $0.1 M_{\odot}$ (blue), and $0.3 M_{\odot}$ (red). Solid and dashed lines distinguish between $\alpha = 0.1$ and 0.01 . The opacity κ is taken as $1 \text{ cm}^2 \text{ g}^{-1}$. The peak luminosity is found to be around $10^{40} \sim 10^{41} \text{ erg s}^{-1}$. Taking a typical case for example, where the parameters are $M_{\text{disc}} = 0.3 M_{\odot}$, $\alpha = 0.1$, and $v_{\text{out}} = 0.1c$, we derive an outflow mass $M_{\text{out}} \approx 0.037 M_{\odot}$. In this case, a peak luminosity $L_{\text{peak}} \approx 10^{41} \text{ erg s}^{-1}$ is obtained, which is in agreement with the three kilonovae associated with GRBs 050709, 060614 (Jin et al. 2015, 2016), and 130603B.

As mentioned above, the ejecta opacity can influence the luminosity significantly. The kilonova AT2017gfo (GW170817) has a peak bolometric luminosity $L_{\text{bol}} \approx 5 \times 10^{41} \text{ erg s}^{-1}$ (Cowperthwaite et al. 2017). In order to explain the peak luminosity of AT2017gfo, higher opacity with $\kappa = 1 \sim 10 \text{ cm}^2 \text{ g}^{-1}$ may be ruled out. Instead, larger M_{out} , v_{out} , and lower κ ($\lesssim 0.5 \text{ cm}^2 \text{ g}^{-1}$) are favoured (Smartt et al. 2017).

4 CONCLUSIONS AND DISCUSSION

In this work, we have extended the limited-energy advection upon NDAFs for the first time, which naturally gives an output of energy. By using this model along with a couple of simplified assumptions,

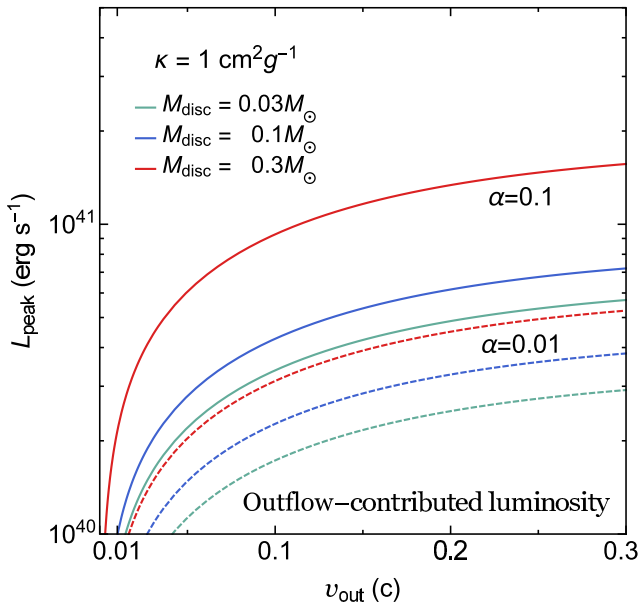


Figure 6. Variation of the peak luminosity L_{peak} with the outflows velocity v_{out} . Three typical disc masses are examined, i.e. $M_{\text{disc}} = 0.03 M_{\odot}$ (green), $0.1 M_{\odot}$ (blue), and $0.3 M_{\odot}$ (red). Solid and dashed lines distinguish between $\alpha = 0.1$ and 0.01 .

the outflows that contribute to kilonova have been examined in a tidy way. In addition, the energy output and the masses of the ejecta have been evaluated. Our results have shown that about $10^{-3} \sim 10^{-1} M_{\odot}$ of the disc mass is launched to the form of outflows, providing the materials and the energy source for the kilonova ejecta. The peak luminosity is estimated to be around $10^{40} \sim 10^{41} \text{ erg s}^{-1}$, from the contribution by outflows.

The outflows of the hyperaccretion discs described by equation (6) are, in fact, taken from the excess of the advection, which is restrained to less than 20 per cent of the total heating energy. But this value is actually quiet uncertain, the possible values can wander from a few per cent up to around thirty percent, due to the variation of the flow density. However, there are strong evidence for the outflows as mentioned in Section 1, so the issue may be the least of our concern.

Gao et al. (2017) presented the merger-nova events from *Swift* SGRBs sample. They have found three candidates GRB 050724, 070714B, and 061006. The optical peak luminosity of these sources is around $10^{42} \sim 10^{43} \text{ erg s}^{-1}$, which is a few tens to hundreds times brighter than the normal kilonova. So the central engine of these candidates must be something different rather than a BH surrounded by a disc. The merger of an NS binary may result in a massive millisecond magnetar, which can continuously provide additional source of energy ejection to power the merger ejecta (Yu et al. 2013; Siegel & Cioffi 2016). An alternative way to explain such high luminosity is by considering the vertical advection effects caused by the magnetic buoyancy (Jiang et al. 2014). Optically thick accretion flows are capable of trapping a significant amount of photons. Those photons together with the in-falling matter, will be devoured by the BH before they can even escape. The vertical advection effect rescues part of these trapped photons, by bringing out them with the bulk motion of the hot flows (Yi et al. 2017). The speed of the vertical advection is roughly the local sound speed in general, much faster than the diffusive speed of the photons. The existence of the outflows is a natural bridge for such energy transportation. An extra part of the radiation can be unleashed through the out-travelling

materials, so the contribution from it will enhance the luminosity to the kilonova.

ACKNOWLEDGEMENTS

We thank Da-Bin Lin, Shu-Jin Hou, and Mou-Yuan Sun for beneficial discussion, and thank the referee for helpful suggestions that improved the manuscript. This work was supported by the National Basic Research Programme of China (973 Programme) under grants 2014CB845800, the National Natural Science Foundation of China under grants 11573023, 11473022, and 11333004, and the CAS Open Research Program of Key Laboratory for the Structure and Evolution of Celestial Objects under grant OP201503.

REFERENCES

- Abbott B. P. et al., 2017a, *Phys. Rev. Lett.*, 119, 161101
 Abbott B. P. et al., 2017a, *ApJ*, 848, L13
 Abbott B. P. et al., 2017b, *ApJ*, 848, L12
 Abbott B. P. et al., 2017b, *ApJ*, 850, L39
 Barnes J., Kasen D., 2013, *ApJ*, 775, 18
 Berger E., 2014, *ARA&A*, 52, 43
 Berger E., Fong W., Chornock R., 2013, *ApJ*, 774, L23
 Blandford R. D., Znajek R. L., 1977, *MNRAS*, 179, 433
 Cao X., Liang E.-W., Yuan Y.-F., 2014, *ApJ*, 789, 129
 Chen W.-X., Beloborodov A. M., 2007, *ApJ*, 657, 383
 Chornock R. et al., 2017, *ApJ*, 848, L19
 Coulter D. A. et al., 2017, *Science*, 358, 1556
 Cowperthwaite P. S. et al., 2017, *ApJ*, 848, L17
 Dai Z. G., Lu T., 1998, *Phys. Rev. Lett.*, 81, 4301
 Dai Z. G., Wang X. Y., Wu X. F., Zhang B., 2006, *Science*, 311, 1127
 Di Matteo T., Perna R., Narayan R., 2002, *ApJ*, 579, 706
 Drout M. R. et al., 2017, *Science*, 358, 1570
 Duncan R. C., Thompson C., 1992, *ApJ*, 392, L9
 Evans P. A. et al., 2017, *Science*, 358, 1565
 Fan Y.-Z., Yu Y.-W., Xu D., Jin Z.-P., Wu X.-F., Wei D.-M., Zhang B., 2013, *ApJ*, 779, L25
 Fender R., Wu K., Johnston H., Tzioumis T., Jonker P., Spencer R., van der Klis M., 2004, *Nature*, 427, 222
 Fernández R., Metzger B. D., 2013, *MNRAS*, 435, 502
 Fernández R., Metzger B. D., 2016, *Annu. Rev. Nucl. Part. Sci.*, 66, 23
 Fernández R., Foucart F., Kasen D., Lippuner J., Desai D., Roberts L. F., 2017, *Class. Quantum Gravity*, 34, 154001
 Fujibayashi S., Kiuchi K., Nishimura N., Sekiguchi Y., Shibata M., 2017, preprint (arXiv:1711.02093)
 Ganguly R., Brotherton M. S., 2008, *ApJ*, 672, 102s
 Gao H., Ding X., Wu X.-F., Dai Z.-G., Zhang B., 2015, *ApJ*, 807, 163
 Gao H., Zhang B., Lü H.-J., Li Y., 2017, *ApJ*, 837, 50
 Gu W.-M., 2012, *ApJ*, 753, 118
 Gu W.-M., 2015, *ApJ*, 799, 71
 Gu W.-M., Liu T., Lu J.-F., 2006, *ApJ*, 643, L87
 Hirose S., Blaes O., Krolik J. H., 2009, *ApJ*, 704, 781
 Jiang Y.-F., Stone J. M., Davis S. W., 2014, *ApJ*, 796, 106
 Jiang Y.-F., Stone J., Davis S. W., 2017, *ApJ*, preprint (arXiv:1709.02845)
 Jin Z.-P., Xu D., Fan Y.-Z., Wu X.-F., Wei D.-M., 2013, *ApJ*, 775, L19
 Jin Z.-P., Li X., Cano Z., Covino S., Fan Y.-Z., Wei D.-M., 2015, *ApJ*, 811, L22
 Jin Z.-P. et al., 2016, *Nat. Commun.*, 7, 12898
 Just O., Bauswein A., Pulpillo R. A., Goriely S., Janka H.-T., 2015a, *MNRAS*, 448, 541
 Just O., Bauswein A., Ardevol Pulpillo R., Goriely S., Janka H.-T., 2015b, preprint (arXiv:1504.05448)
 Kasen D., Badnell N. R., Barnes J., 2013, *ApJ*, 774, 25
 Kasen D., Fernández R., Metzger B. D., 2015, *MNRAS*, 450, 1777
 Kawaguchi K., Kyutoku K., Shibata M., Tanaka M., 2016, *ApJ*, 825, 52
 Kawanaka N., Kohri K., 2012, *MNRAS*, 419, 713

- Kawanaka N., Piran T., Krolik J. H., 2013, *ApJ*, 766, 31
- Kohri K., Mineshige S., 2002, *ApJ*, 577, 311
- Kohri K., Narayan R., Piran T., 2005, *ApJ*, 629, 341
- Li X., Hu Y.-M., Jin Z.-P., Fan Y.-Z., Wei D.-M., 2017, *ApJ*, 844, L22
- Li L.-X., Paczyński B., 1998, *ApJ*, 507, L59
- Liu T., Gu W.-M., Xue L., Lu J.-F., 2007, *ApJ*, 661, 1025
- Liu T., Hou S.-J., Xue L., Gu W.-M., 2015, *ApJS*, 218, 12
- Liu T., Gu W.-M., Zhang B., 2017, *New Astron. Rev.*, 79, 1
- Liu H.-J., Zhang B., Lei W.-H., Li Y., Lasky P. D., 2015, *ApJ*, 805, 89
- Metzger B. D., 2017, *Living Rev. Relativ.*, 20, 3
- Metzger B. D., Berger E., 2012, *ApJ*, 746, 48
- Metzger B. D. et al., 2010, *MNRAS*, 406, 2650
- Metzger B. D., Giannios D., Thompson T. A., Bucciantini N., Quataert E., 2011, *MNRAS*, 413, 2031
- Murguía-Berthier A. et al., 2017a, *ApJ*, 835, L34
- Murguía-Berthier A. et al., 2017b, *ApJ*, 848, L34
- Nakar E., 2007, *Phys. Rev.*, 442, 166
- Narayan R., Paczynski B., Piran T., 1992, *ApJ*, 395, L83
- Narayan R., Piran T., Kumar P., 2001, *ApJ*, 557, 949
- Ohsuga K., 2007, *ApJ*, 659, 205
- Paczynski B., Wiita P. J., 1980, *A&A*, 88, 23
- Perego A., Rosswog S., Cabezón R. M., Korobkin O., Käppeli R., Arcones A., Liebendörfer M., 2014, *MNRAS*, 443, 3134
- Popham R., Narayan R., 1995, *ApJ*, 442, 337
- Popham R., Woosley S. E., Fryer C., 1999, *ApJ*, 518, 356
- Potter W. J., Balbus S. A., 2014, *MNRAS*, 441, 681
- Pounds K. A., Reeves J. N., 2009, *MNRAS*, 397, 249
- Proga D., 2003, *ApJ*, 585, 406
- Rosswog S., 2015, *Int. J. Mod. Phys. D*, 24, 1530012-52
- Samadi M., Abbassi S., 2016, *MNRAS*, 455, 3381
- Shakura N. I., Sunyaev R. A., 1973, *A&A*, 24, 337
- Shen Z.-Q., Jin Z.-P., Liang Y.-F., Li X., Fan Y.-Z., Wei D.-M., 2017, *ApJ*, 835, L22
- Shibata M., Fujibayashi S., Hotokezaka K., Kiuchi K., Kyutoku K., Sekiguchi Y., Tanaka M., 2017, *Phys. Rev. D*, 96, 123012
- Siegel D. M., Cioffi R., 2016, *ApJ*, 819, 15
- Siegel D. M., Metzger B. D., 2017, *Phys. Rev. Lett.*, 119, 231102
- Smartt S. J. et al., 2017, *Nature*, 551, 75
- Song C.-Y., Liu T., Gu W.-M., Hou S.-J., Tian J.-X., Lu J.-F., 2015, *ApJ*, 815, 54
- Song C.-Y., Liu T., Gu W.-M., Tian J.-X., 2016, *MNRAS*, 458, 1921
- Sądowski A., Narayan R., 2015, *MNRAS*, 453, 3213
- Sądowski A., Narayan R., 2016, *MNRAS*, 456, 3929
- Tanaka M., 2016, *Adv. Astron.*, 2016, 634197
- Tanaka M., Hotokezaka K., 2013, *ApJ*, 775, 113
- Tanaka M. et al., 2017, *PASJ*, 69, 102
- Tanvir N. R., Levan A. J., Fruchter A. S., Hjorth J., Hounsell R. A., Wiersema K., Tunnicliffe R. L., 2013, *Nature*, 500, 547
- Terashima Y., Wilson A. S., 2001, *ApJ*, 560, 139
- Usov V. V., 1992, *Nature*, 357, 472
- Wang Q. D. et al., 2013, *Science*, 341, 981
- Xie W., Lei W.-H., Wang D.-X., 2016, *ApJ*, 833, 129
- Xue L., Liu T., Gu W.-M., Lu J.-F., 2013, *ApJS*, 207, 23
- Yi T., Gu W.-M., Yuan F., Liu T., Mu H.-J., 2017, *ApJ*, 836, 245
- Yuan F., Bu D., Wu M., 2012, *ApJ*, 761, 130
- Yuan F., Wu M., Bu D., 2012, *ApJ*, 761, 129
- Yu Y.-W., Zhang B., Gao H., 2013, *ApJ*, 776, L40
- Zalamea I., Beloborodov A. M., 2011, *MNRAS*, 410, 2302

This paper has been typeset from a \LaTeX file prepared by the author.